Arabian Journal for Science and Engineering
https://doi.org/10.1007/s13369-024-08865-2

RESEARCH ARTICLE-MECHANICAL ENGINEERING

Tribological and Structural Effects of Titanium Carbide and Hexagonal Boron Nitride Reinforcement on Aluminum Matrix Hybrid Composites

Merve Horlu[1] · Cevher Kursat Macit[2] · Bunyamin Aksakal[2] · Burak Tanyeri[2]

Received: 12 September 2023 / Accepted: 12 February 2024

Abstract
This research involves the synthesis of a hybrid composite by adding titanium carbide (TiC) and hexagonal boron nitride (hBN) powders in certain weight ratios (2.5–5%) to pure aluminum (Al) powder. When previous studies were examined, it was seen that TiC and hBN powders were added separately to Al matrix powders; however, a hybrid composite was not produced as in this study. The obtained hybrid composites were characterized by scanning electron microscopy (SEM), energy dispersive spectroscopy (EDX) and X-ray diffraction (XRD) analysis. Microstructure, hardness and wear tests were carried out under 3 different loads (10 N, 20 N and 30 N) and dry conditions. Weight loss and coefficient of friction measurements were obtained for each hybrid composite during the wear tests. The TiC–hBN-reinforced specimen exhibited a significantly higher hardness value of 37.08% compared to the pure Al composite. It was also found that the synthesized Al–TiC–hBN hybrid composite exhibited a 59% reduction in the wear loss value for 10 N load, 30% for 20 N load and 60% for 30 N load compared to the pure Al sample. It is believed that the hybrid composites produced in this study have the ability to compete with Al matrix materials and exhibit the potential for longer durability and cost reduction in industries that use the production of aluminum parts.

Keywords Aluminum · Metal matrix hybrid composite · Hexagonal boron nitride · Titanium carbide · Wear

1 Introduction

The primary objectives of technological advancements are centered around enhancing living conditions, with a significant emphasis placed on the development and production of more efficient and functional materials. [1, 2]. Since the second half of the twentieth century, research and studies in materials science have accelerated with the emergence of metal matrix composites (MMC) [3]. MMCs are recognized as one of the most suitable material groups in various engineering applications and industrial fields due to their superior properties compared to conventional materials [4]. Aluminum (Al) is the most widely used and preferred metal matrix composite, because it is a recyclable, highly formable, lightweight material with good electrical and thermal conductivity [5, 6]. Due to such advantages, aluminum (Al) and its alloys are widely utilized in several industries including aviation, defense, space, and automotive sectors. [7]. Nevertheless, the primary drawbacks associated with aluminum alloys are their limited wear resistance and mechanical qualities at high temperature conditions. In order to mitigate these limitations, several experiments have been conducted to investigate the incorporation of distinct reinforcing materials into aluminum and its alloys. Because the addition of reinforcing elements improves the mechanical, tribological, structural, and thermophysical properties of Al and its alloys, research on Al and its alloys remains up to date. [5–7].

Powder metallurgy (PM), along with other production methods, is a commonly used technology in the manufacture of composite materials, being one of the primary metal matrix production processes. Because some metals are difficult to produce using other processes, the PM approach can shape them at a lower cost. PM-shaped parts are manufactured as final products and used in aerospace, automotive, defense, electronics, and other areas [8, 9]. Al and its alloys are the most popular composite materials made by PM due

✉ Merve Horlu
mervehorlu@gmail.com

[1] Department of Mechanical Engineering, Technology Faculty, Firat University, Elazig, Turkey

[2] Aircraft Airframe-Engine Maintenance, School of Aviation, Firat University, Elazig, Turkey

Published online: 11 March 2024

to their inexpensive cost, light weight, and ease of processing. Furthermore, the desired mechanical properties can be obtained by adding different reinforcing elements to these powdered materials. Due to their excellent mechanical characteristics such as low density, high hardness, high strength, and good chemical stability, the use of B4C, SiC, TiC, and Al2O3 has been increasing. [10, 11].

Engineering materials are subjected to varying loads and moments under various operating situations, where low wear resistance is undesirable. Since the increase in temperature in frictional materials causes wear, the friction factor is an important parameter in interacting materials [12]. As a result of the local relationship between the interaction surfaces of materials, wear can be defined as the loss of material during relative motion [13]. Materials in contact with each other and subjected to wear, where high wear resistance is required depending on the working conditions. To reduce wear, research on various composite materials, such as PM materials with various reinforcements and coated materials, is presently ongoing. [14].

Because of its high hardness, melting point temperature, and modulus, TiC has been selected as a reinforcing material in this study. [15]. Since TiC reinforcing particles are resistant to plastic deformation, it was demonstrated that the plastic deformation or material loss of composites diminishes as TiC reinforcement rises. TiC particles were added to copper matrix composites in another investigation. [16] And it was observed that the hardness and strength of the Cu-TiC composite increased with the addition of TiC in the matrix phase [17]. It has been reported in literature studies that TiC powders should be used to produce metal matrix composites to obtain high mechanical and tribological performance due to their high hardness [18–21].

In contrast to previous research, hexagonal boron nitride (hBN) was used in this study, giving non-toxic and greasy features while appearing structurally comparable to graphite and alumina as well as having the lowest density among ceramic materials (2.27 g/cm^3). hBN has a crystalline structure comparable to graphite, but it has a higher electrical resistance and products made of hBN can be easily machined. [22, 23]. Furthermore, hBN is an inert material, non-chemically reactive, non-toxic, and resistant to very high temperatures. It can also be used in normal atmosphere up to 1000 °C, in vacuum up to 1400 °C, in argon atmosphere up to 2000 °C and in nitrogen atmosphere up to 2400 °C. In addition to being stable against thermal shocks, it has excellent electrical insulation, good thermal conductivity, and UV reflectivity, as well as excellent lubricity. It was also reported that the hBN-containing coatings produce a hard and wear-resistant surfaces enabling to minimize friction by providing good lubricating role at high temperatures up to 800 °C [24]. Recently, hBN has been used as reinforcement to a variety of metals to enhance their mechanical and tribological characteristics. [25, 26]. Hexagonal boron nitride (hBN) was prepared by the molybdenum disulfide (MoS_2) powder metallurgy method and doped to reduce friction in SS316L composites [23]. The addition of carbides and borides has been reported to possess a notable impact on enhancing the wear resistance of aluminum. This is primarily attributed to the extensive reinforcing of aluminum, a soft and ductile material, which effectively reduces the extent of wear-induced deformation in subsurface areas. [27–36].

Table 1 Powder purity and particle sizes used during composite synthesizing

Material	Al	TiC	hBN
Purity (%)	99.9%	%99,9	%99.9
Melting temperatures (C°)	650	3067	2000
Particle size (μm)	0 < Al < 50	0 < TiC < 50	0 < hBN < 50
Brand	Sigma-Aldrich	Sigma-Aldrich	Sigma-Aldrich

When the literature studies are examined, there are studies in which TiC and hBN powders are added to Al powders separately. However, it was observed that a hybrid combination was not produced as realized in this study. In this study, a new hybrid composite was made by utilizing the individual properties of TiC and hBN. With this new composite, it is aimed to increase the mechanical properties of TiC reinforcement and to increase the wear properties of hBN thanks to its lubricating properties. In this research, the addition of TiC and hBN powders to pure aluminum powder was carried out through a hybrid mechanical mill. The microstructure of the composite samples was investigated using scanning electron microscopy (SEM), energy-dispersive X-ray spectroscopy (EDX) and X-ray diffraction (XRD). In addition, the hardness and wear properties of the materials were evaluated under dry conditions with three different loads (10 N, 20 N and 30 N).

2 Materıals and Methods

2.1 Chemical Properties and Nomenclature of Al–TiC–hBN Powders

The particle sizes and physical properties of the powders used in the study are shown in Table 1, and the number of samples used by weight in the powders produced and the nomenclature of the composites are shown in Table 2. The

Table 2 Hybrid composite groups and compositions

Sample	Al	TiC	hBN
Al	%100	–	–
Al–TiC	%95	%5	–
Al–hBN	%95	–	%5
Al–TiC–hBN	%95	%2.5	%2.5
Al–3TiC–2hBN	%95	%3	%2
Al–2TiC–3hBN	%95	%2	%3

processes to be carried out in the study are shown in Fig. 1.

2.2 Preparation of Al–TiC–hBN Powders

During the synthesizing of composite materials, the mixing ratios were first determined as shown in Table 2. Then, the powders weighed with a precision balance (Precisa) and were mixed in a mechanical mixer at 250 rpm for 30 min. Steel balls with a diameter of 6 mm were used in the mechanical grinder. The powders, whose particle sizes were selected close to each other, were mixed homogeneously. The schematic illustration of preparation process of Al–TiC–hBN hybrid powders is shown in Fig. 2.

2.3 Preparation of Al–TiC–hBN Samples

After mixing process, the mixed compounds were pressed in a hydraulic cold press. The inside of the mold was lubricated with $Zn(C_{18}H_{35}O_2)_2$ (Zinc stearate) to remove the powders more easily from the mold after pressing. The pressing process was carried out at a pressure of 50 MPa and the sintering

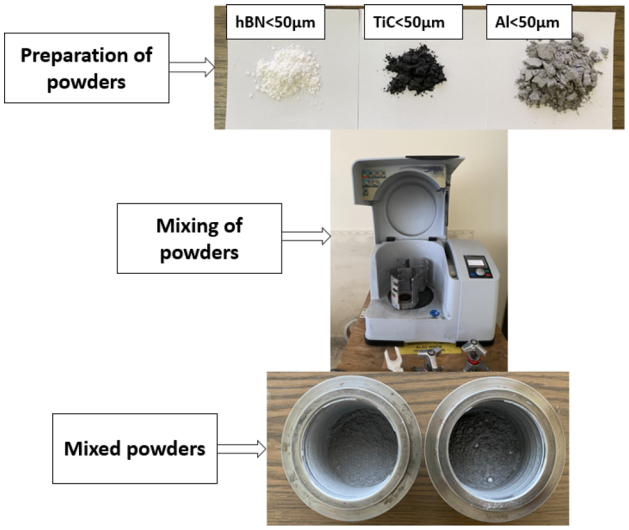

Fig. 2 Preparation and mixing of the powders

process was carried out at 600 °C, close to the melting temperature of aluminum, under an atmosphere of high purity nitrogen (Linde – 99.999%) in a 316L stainless steel tube furnace with temperature control by Honeywell DC 2500 controller. The preparation process of Al–TiC–hBN hybrid composite samples is shown in Fig. 3.

2.4 Determination of Density of Composites

The density of the produced composites was calculated experimentally using Archimedean principle [39–41]. Deionized water was selected as the immersion liquid. A balance with a precision of 10^{-5} (Shimadzu AUW-220D) was

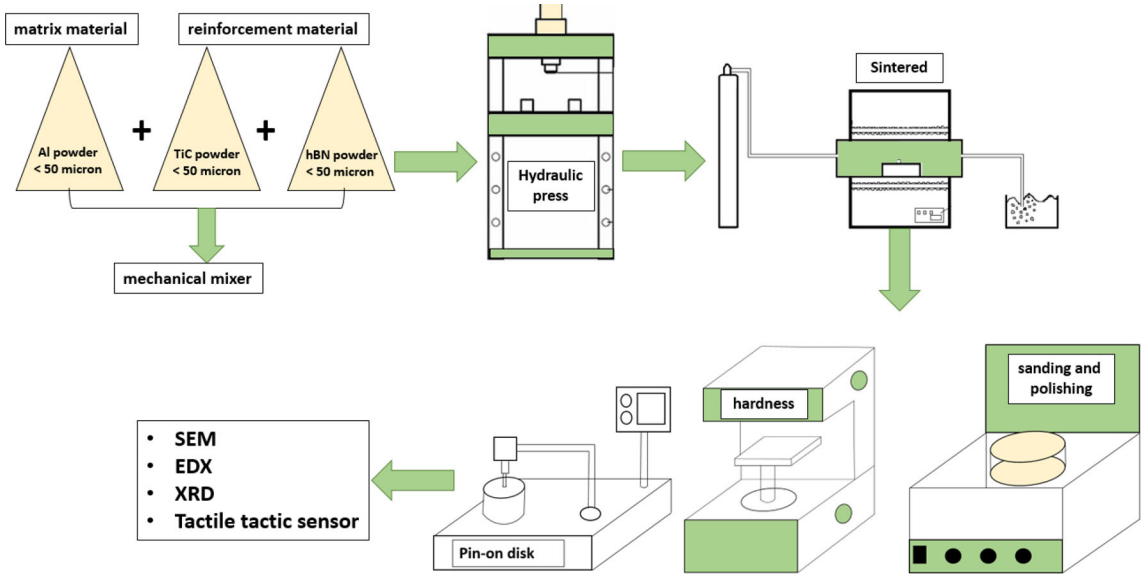

Fig. 1 Process flow chart during synthesizing the hybrid composites

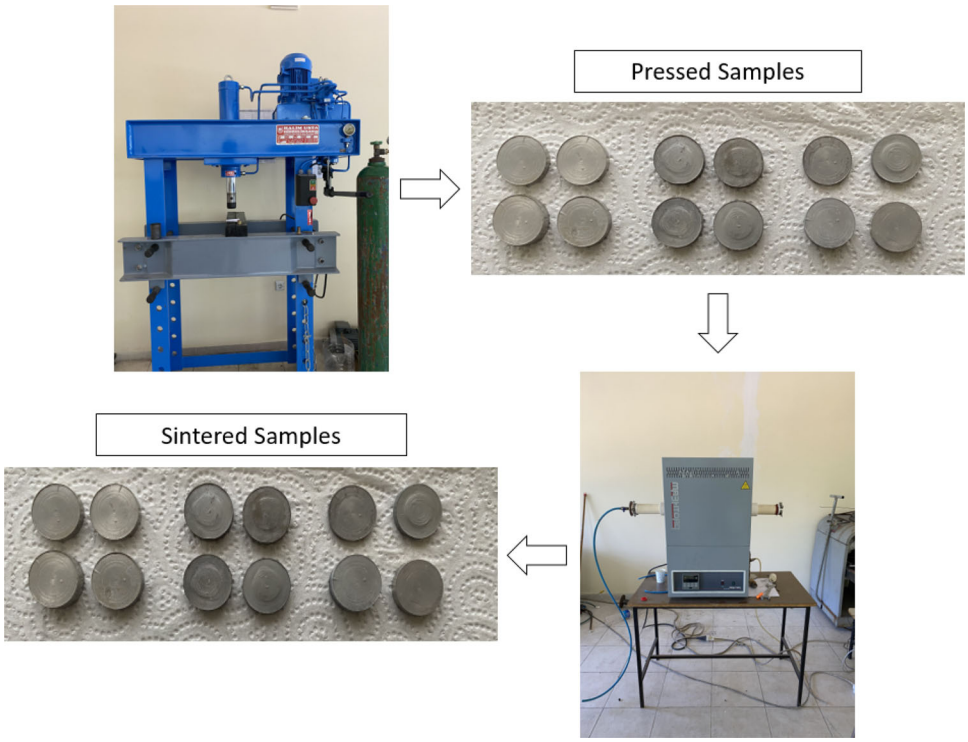

Fig. 3 Preparation of cold-pressed and sintered composite disks

used to weigh all samples. The average value of three values obtained under the same conditions of all test samples was reported. The following equations were used to calculate the experimental density and the theoretical density [37–39].

$$\text{Experimental density}\left(\text{g/cm}^3\right) = \rho_e = \frac{W_a \rho_w}{W_a - W_w} \tag{1}$$

$$\text{Theoretical density}\left(\text{g/cm}^3\right) = \frac{\text{Total mass}}{\text{Total volume}} = \frac{\text{Al mass} + \text{hBN mass} + \text{TiC mass}}{\left(\frac{\text{Al mass}}{\text{Al density}}\right) + \left(\frac{\text{hBN mass}}{\text{hBN density}}\right) + \left(\frac{\text{TiC mass}}{\text{TiC density}}\right)} \tag{2}$$

where ρ_e, W_a, ρ_w, W_w are the observed density (g/cm^3), weight of the samples in air, water density and weight of the sample in water, respectively [38–40].

2.5 Microstructure and Characterization of Hybrid Composites

The sintering process was completed and the samples were taken into bakelite before microstructure and microhardness tests were performed. Sanding and polishing were carried out to examine the microstructures of the samples more clearly after the bakelitizing process was completed. The processes were carried out on SiC sandpapers of 100, 240, 400, 600, 800, 1000, and 1200 mesh, respectively, and then were polished with a 3 μm diamond paste. The samples were also washed with alcohol after polishing. The phase distribution and structural defects of the samples were examined by using an optical microscope (Nikon Eclipse MA100). To examine the wear surfaces more detailed analysis of the samples was performed using SEM and EDX (Zeiss EVO MA10 SEM) to determine the reinforcing element particles distributed in the Al matrix structure. For phase identification of the prepared samples, X-ray diffraction (XRD) was performed on a Rigaku RINT-2000 X-brand instrument with a scan range of $2\theta = 10°$ to 80° and 40 kV/40 mA.

2.6 Hardness

In hardness tests, measurements were taken from 5 different points with a hardness tester at the HV30 hardness unit with a loading time of 15 s, and the average hardness values of the hybrid composites were determined by averaging these values.

2.7 Wear Tests

Wear tests were carried out by a pin-on-disk wear tester (Fig. 4) under dry wear conditions with 3 different loads (10 N, 20 N, and 30 N) at a sliding speed of 50 mm/sec and a total sliding distance of 1000 m using a steel wear pin. At a total sliding distance of 1000 m, the weight losses of the samples were measured at every 100 m on a balance with a sensitivity value of 10-5 (Shimadzu AUW-220D), and the measured values were recorded and weight losses were plotted for each sample with respect to the distance. For the determination of

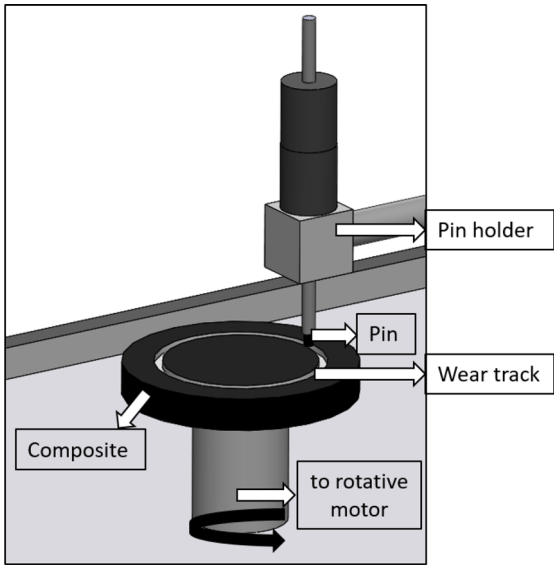

Fig. 4 Pin-on-disk test rig

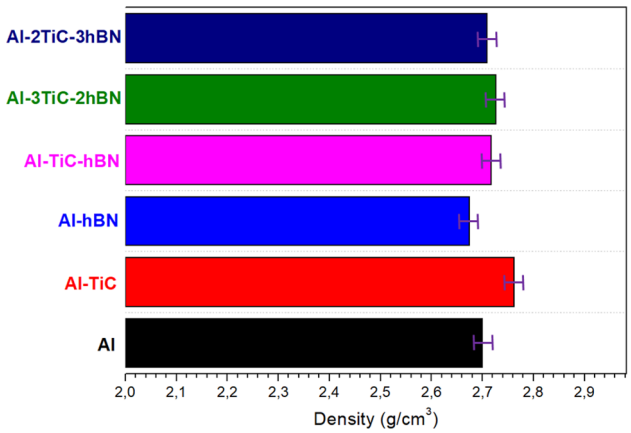

Fig. 5 Calculated density (g/cm^3) values of produced hybrid composites

friction coefficients, each sample was abraded for a sliding distance of 1000 m and the friction coefficient values of the composites were recorded by the wear tester. The recorded coefficient of friction values was then uploaded to the computer and finally coefficient of friction graphs was generated.

3 Results and Discussion

3.1 Density

The densities of the hybrid composites are shown in Fig. 5. It was detected that TiC reinforcement has increased the density value, but the density values decreased with hBN reinforcement. Similar results were also obtained for TiC and hBN reinforcements in literature studies [23–30].

3.2 Microstructure

Optical microscope (OM) images taken at different sizes of the hybrid composite prepared for microstructure examination are shown in Fig. 6. From the plots, it is seen that TiC and hBN particles with close particle sizes are homogeneously distributed in the Al matrix structure.

3.2.1 Optical Microscope Images

Optical microscope images of sanded and polished hybrid composites in 2 different magnifications (100–1000 KX) are shown in Fig. 6. In the optical images, it is observed that the reinforcement powders are homogeneously distributed in the Al structure. In the OM images taken after sintering, thin boride layers were found at the grain boundaries of the sintered Al/hBN composites. It was clearly observed that the boride phase thickened at the grain boundaries with increasing hBN content.

3.2.2 XRD Characterization

XRD analysis results of the hybrid composites prepared for microstructure analysis are shown in Fig. 7. As seen from the patterns, the presence of distinct peaks corresponding to TiC and hBN was detected within the structural composition of the Al matrix. In addition, peaks of aluminum titaniums (Al_3Ti) and (Al_3Ti_2), aluminum boron (AlB_{12}), aluminum nitride (AlN), titanium nitride (Ti_2N) and boron nitride ($B_{25}N$) compounds were observed together with the reinforcing elements and matrix material. The peaks at 2θ values of 38.12°, 44.41°, 64.72°, 77.85° and 81.99° belong to aluminum with Miller indices of (111), (002), (022), (113) and (222), respectively. When the Miller indices are analyzed, the peaks at (002) and (011) with 2θ values of 26.65° and 43.66° correspond to the hexagonal boron nitride structure [25, 26]. In XRD analyses, the indices (111), (200), (220) and (311) represent TiC particles, which vary at 2θ degrees of 36.32°, 41.83°, 61.07° and 75.81° and hkl about (111), (200), (220) and (311). These peaks indicate that TiC particles are homogeneously distributed in the Al matrix [32, 36]. The diffraction peaks of TiC and hBN particles have lower intensities, which can be attributed to the low wt% of hBN and TiC phases in aluminum hybrid composites. Each of the hBN and TiC phases combines strongly with Al particles after sintering through the formation of good bonds between them, improving the physical and mechanical properties.

3.2.3 SEM Images

SEM images obtained in the microstructures of the hybrid composites and EDX mapping results obtained to examine the homogeneity of the reinforcing elements are shown

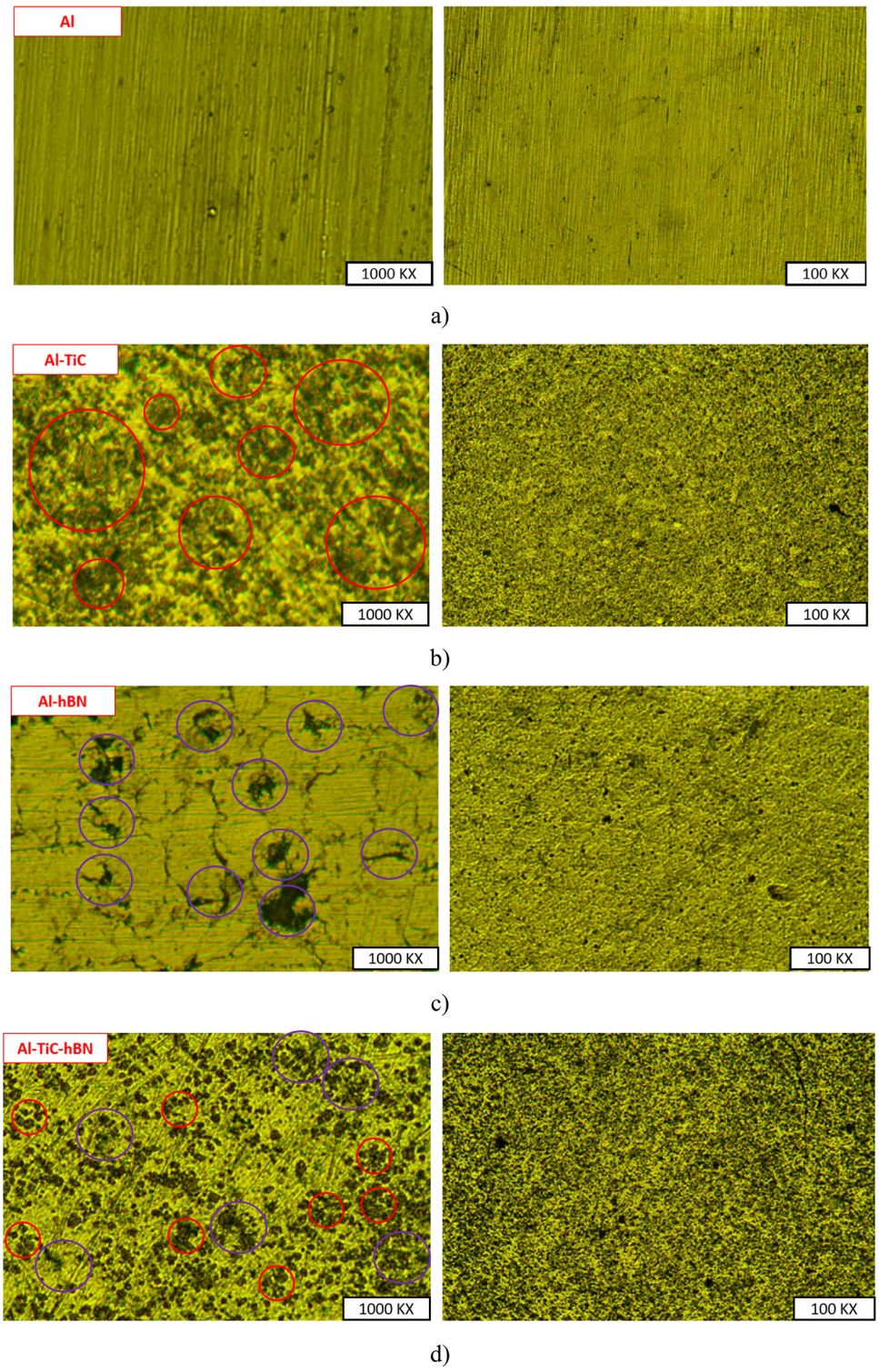

Fig. 6 Microstructure images of hybrid composites; **a** Al, **b** Al–TiC, **c** Al–hBN, **d** Al–TiC–hBN, **e** Al–3TiC–2hBN, **f** Al–2TiC–3Hbn

Fig. 6 continued

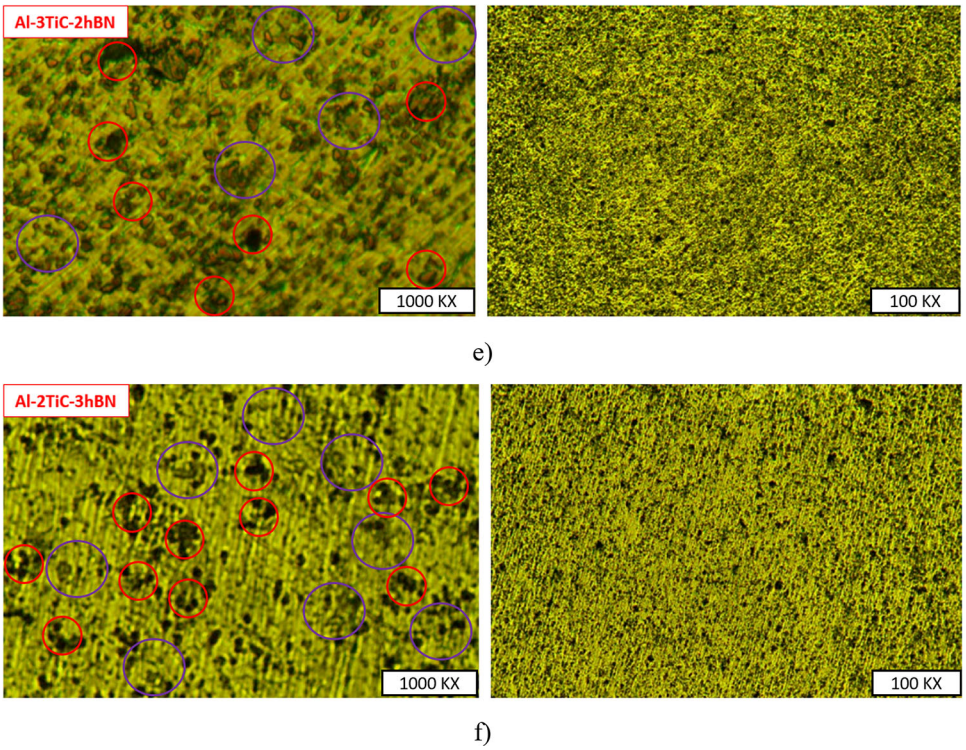

in Figs. 8 and 9. In the EDX results, results similar to the reinforcement amounts in Table 1 were obtained and it was seen that the reinforcing elements were homogeneously distributed in the matrix structure. In the EDX analysis results, it was seen that values close to the doped reinforcing elements given in Table 2. In the examination of the reinforcement particles in the matrix structure by mapping technique, it is seen that hBN and TiC reinforcements are homogeneously distributed in the matrix structure. Although heterogeneity is observed in some sections, this is thought to be due to the chosen reinforcement particle sizes.

3.3 Hardness

Images of the pyramids obtained in hardness tests are shown in Fig. 10, and the results taken from 5 different points of the composites are given in Fig. 11. According to the results obtained in hardness tests, superior results were obtained in all samples compared to pure Al composite. The hardness values of the pure Al sample were similar to the literature studies [41–43]. The highest hardness value was obtained in the Al-TiC-hBN sample and an increase in hardness value of approximately 37.08% was observed compared to the pure Al sample. When the literature studies are examined, it is reported that TiC and hBN powders increase the hardness values of the matrix material [30–34]. The hardness values are highly dependent on the particle size and concentration of the additive particles. The hardness of Al/hBN hybrid composites is higher than that of Al/TiC hBN hybrid composites; hence, hBN reinforcing particles form stronger bonds with Al particles than TiC reinforcing particles, which subsequently inhibit the movement of dislocations and consequently increase the hardness as shown in Fig. 11.

3.4 Wear

The wear weight loss graphs of the samples under 3 different loads are shown in Fig. 12. In wear tests, the tendency of high wear depth increases with increasing load, and similar results were obtained with literature studies [44, 45]. The wear rate of Al/hBN and Al/TiC hybrid composites is highly dependent on the reinforcing particles and their concentration. The increase in the wt% of hBN and TiC leads to a decrease in wear rate (increase in wear resistance), which is due to bonding at the interfaces between the reinforcing particles and Al particles, which then creates thermal stresses at the interfaces. The differences between the melting points of the reinforcing nanoparticles and aluminum particles and subsequently these thermal stresses will increase the interlocking of the dislocations. The reinforcing particles will inhibit the movement of dislocations and increase wear resistance (reduce the wear rate).

It is also supported by literature studies that TiC additive positively affects the wear resistance of composites in the samples where wear tests were performed [46–49]. The resistance on the wear surfaces of the samples is attributed

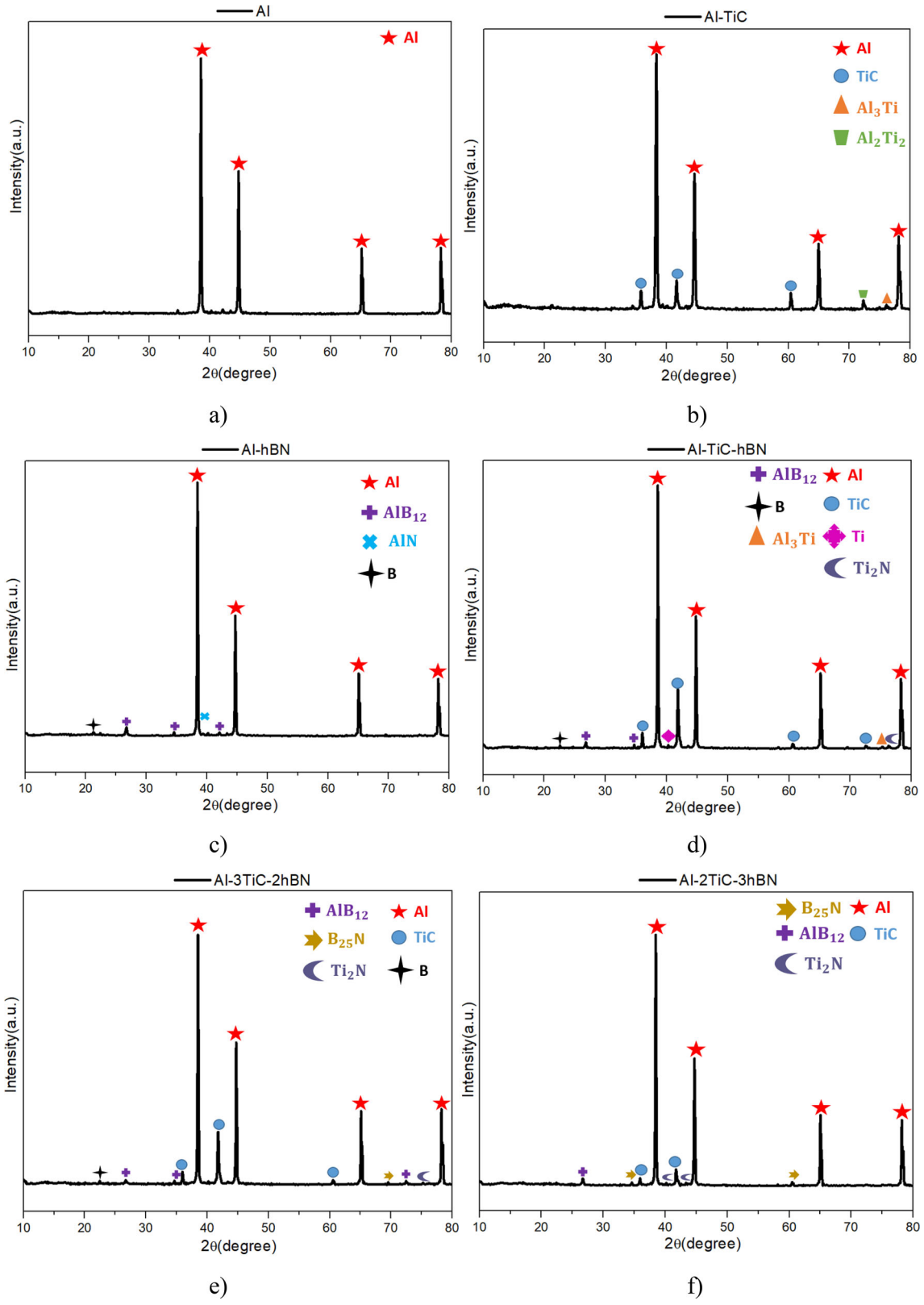

Fig. 7 XRD diffraction patterns **a** Al, **b** Al–TiC, **c** Al–hBN, **d** Al–TiC–hBN, **e** Al–3TiC–2hBN, **f** Al–2TiC–3hBN

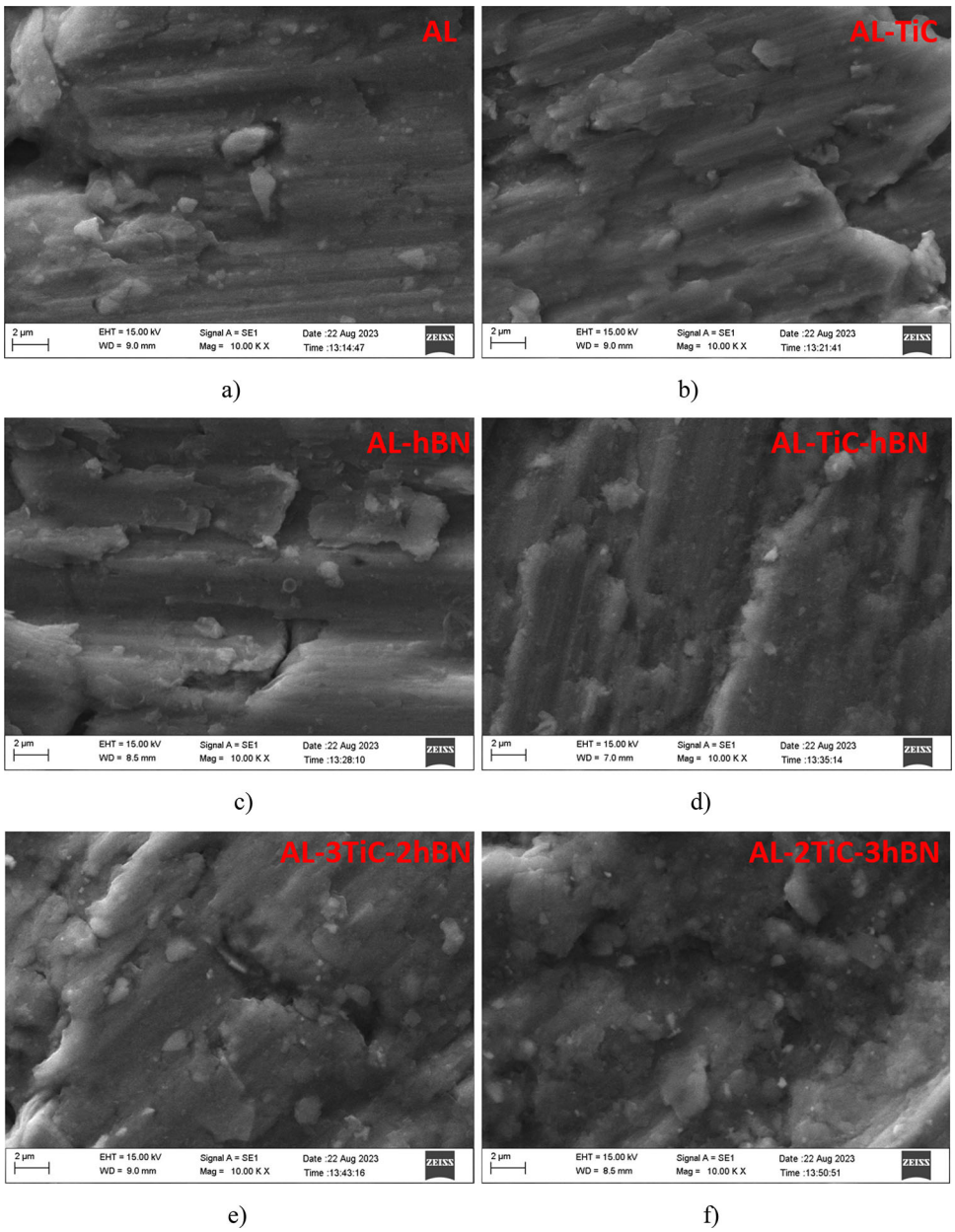

Fig. 8 SEM views of hybrid composites; **a** Al, **b** Al–TiC, **c** Al–hBN, **d** Al–TiC–hBN, **e** Al–3TiC–2hBN, **f** Al–2TiC–3hBN

to the improvement of the hardness where significant interfacial bonds between the matrix and ceramic particles, the embedding of hard TiC particles, the grain refinement in the structure, and the hBN particles [47, 48]. The reduction in the wear rate of the composites is thought to be due to the effective formation of a tribo-layer, which becomes thicker and denser as the weight % of hBN increases [25]. At the same time, the increase in wear resistance of the composites was attributed to the presence of hBN reinforcement with solid lubricant properties. hBN particles are thought to form a protective layer between the matrix and the surface material and reduce the wear rate [24–26]. When the rate of weight loss as a result of wear is examined, the lowest weight loss was obtained in the Al–TiC–hBN composite and a 59% decrease for 10 N, 30% for 20 N, and 60% for 30 N were obtained, respectively, compared to the pure Al sample. The increase in applied loads also increased the amount of wear for all samples.

Friction coefficient graphs recorded as a result of wear tests (10 N) and average friction coefficient values obtained from the wear tester as a result of 3 different loads are shown in Fig. 13. Decreases in friction coefficient values were observed with the effect of reinforcements and such values are supported by literature studies [23–26, 34]. In addition, due to the layered hexagonal crystal structure of hBN particles, a thin lubricating film is formed on the pin surface

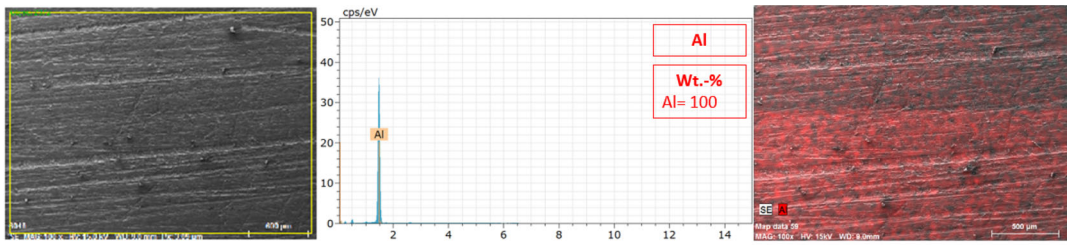

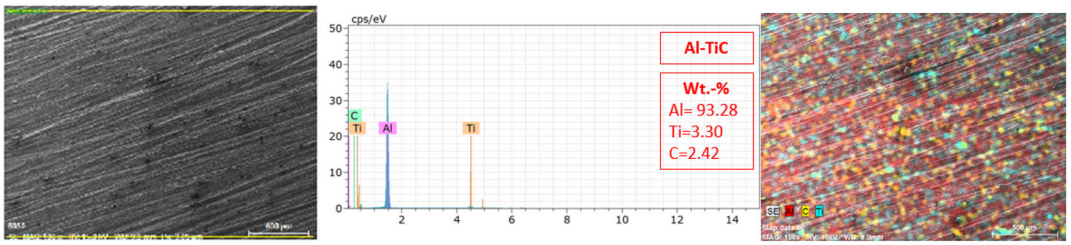

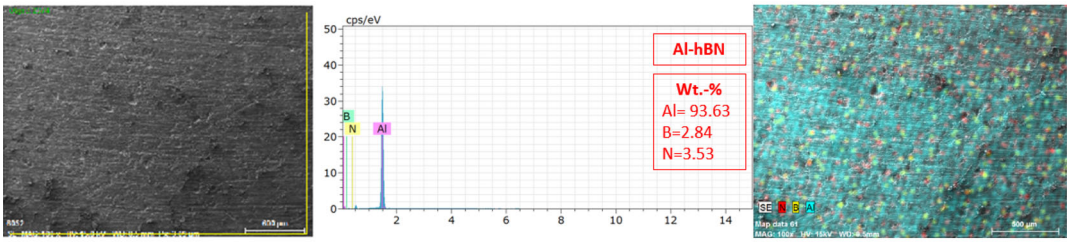

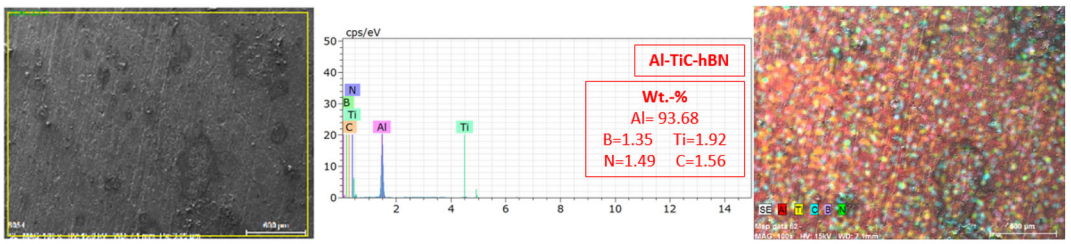

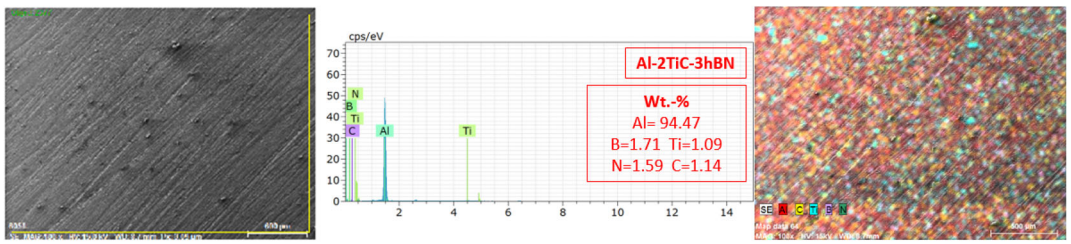

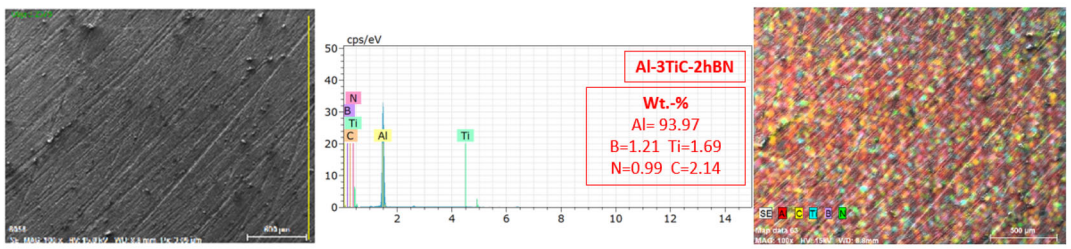

Fig. 9 EDX spectra of synthesized hybrid composites **a** AL, **b** Al–TiC, **c** Al–hBN, **d** Al–TiC–hBN, **e** Al–3TiC–2hBN, **f** Al–2TiC–3hBN

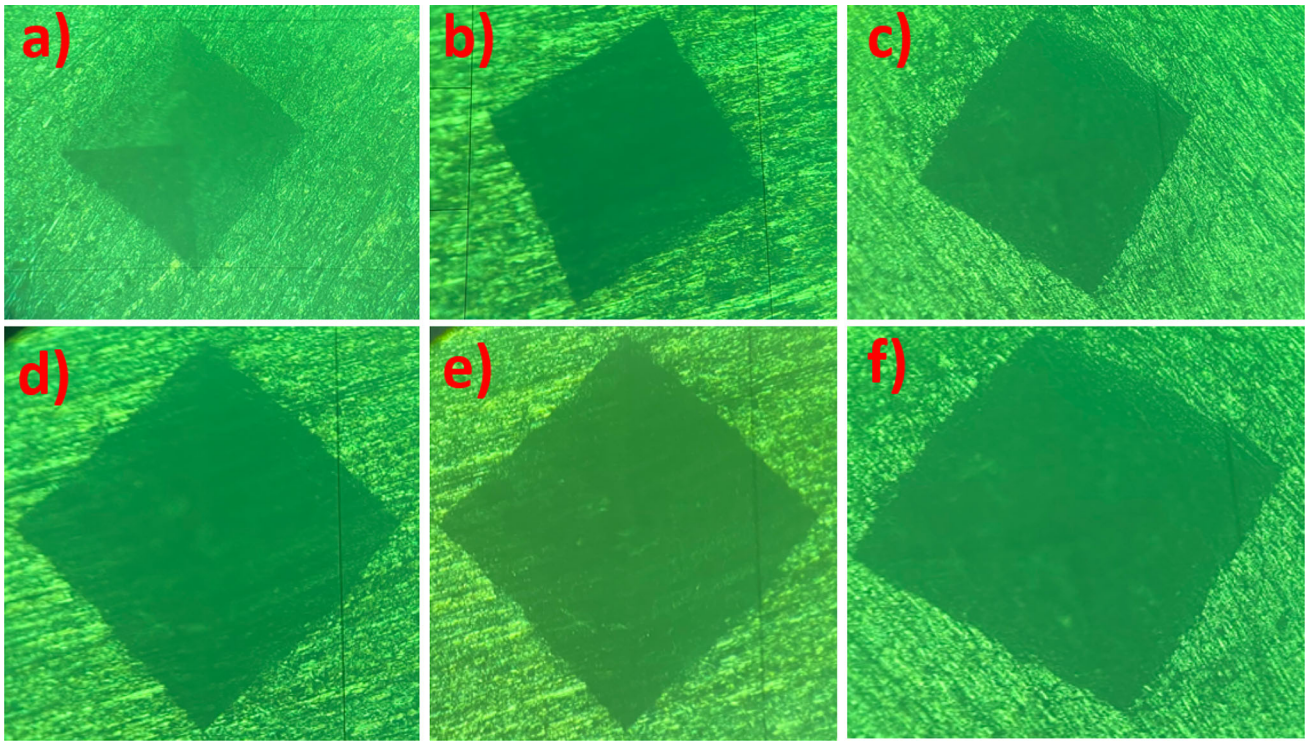

Fig. 10 Various sample images of hardness indentation **a** AL, **b** Al–TiC, **c** Al–hBN, **d** Al–TiC–hBN, **e** Al–3TiC–2hBN, **f** Al–2TiC–3hBN

of the composites during pure sliding wear, which is thought to be the main reason for the decrease in COF by adding hBN to the composite [26]. Similar to the hardness and weight loss results for the coefficient of friction values, the lowest coefficient of friction was obtained for the Al–TiC–hBN composite. When the friction coefficient graphs were examined in detail, it was observed that the friction coefficient value increased intensely in the pure Al sample as the wear continued in the cracked areas for a long time, while the friction coefficient value remained constant for a certain period of time with the TiC reinforcement, and the friction resistance decreased visibly in the graphs with the formation of the tribo-layer.

From the literature studies, where reinforcing elements have been used previously, sintered composites with hBN content of 10 and 15% by volume in stainless steels showed higher coefficients of friction than the sintered composite with 20% h-BN by volume [23]. The amount of hBN in composites can be optimized to reduce friction depending on the hBN loading. For example, increasing the hBN content from 0 to 10 wt% in Cu-based composite and adding 4.0 wt% hBN to Ni-based composite resulted in slight increases in friction [50, 51].

As a result of wear tests under 3 different loads, SEM images of the hybrid composites after wear at the lowest (10 N) and the highest (30 N) forces are shown in Figs. 14 and 15. In the SEM images, it was observed that deep cracks and

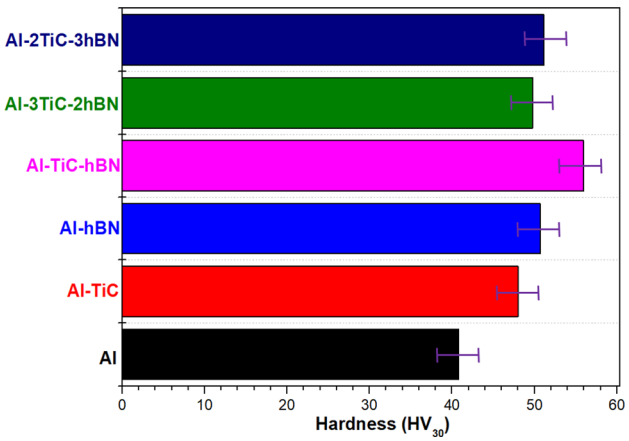

Fig. 11 Hardness values for the produced hybrid composites

large gaps were formed in the pure Al sample as a result of wear. With TiC and hBN reinforcement, there is a noticeable decrease in wear tracks and wear path diameter. This is thought to be due to the resistance of the reinforcements against wear. It was observed that hBN reinforcement forms a tribo-layer on the surface of the samples against wear and reduces the direct metal-to-metal contact. TiC particles were also homogeneously dispersed against wear, reducing the wear depth and scars. In SEM images shown in Figs. 14 and 15, it can also observe that TiC and hBN particles increased the adhesion friction on the wear track. Adhesive and abrasive

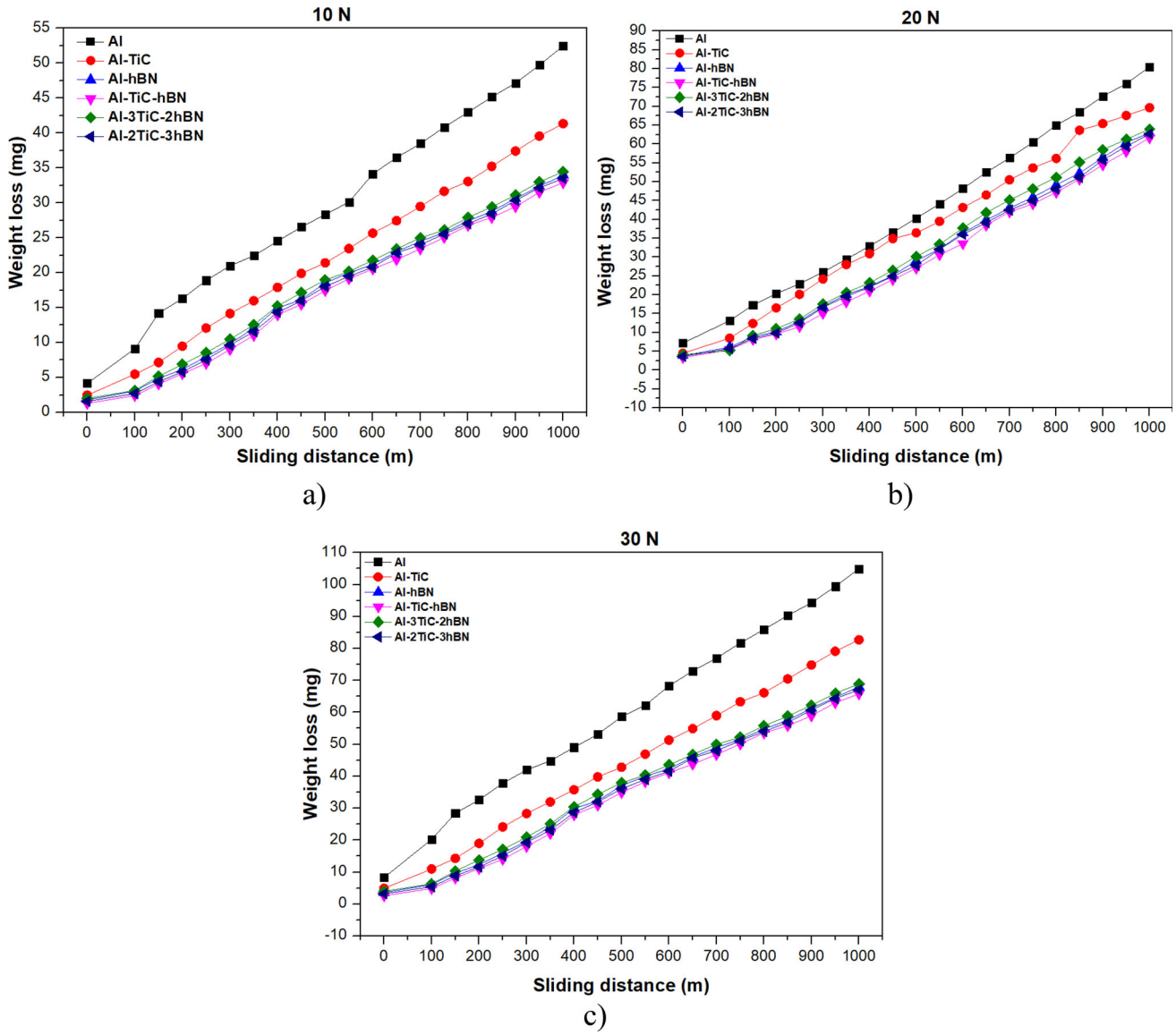

Fig. 12 Change in weight losses with sliding distance (mg) for **a** 10 N, **b** 20 N, **c** 30 N loadings

wear was generated for all samples. At low loads, abrasive wear is the main wear mechanism, while at higher loads, adhesive wear is the main wear mechanism. The grooves of Al/hBN hybrid composites are thinner than the grooves of Al/TiC hybrid composites because hBN particles showed a better wear resistance than TiC particles due to the increase in temperature in the wear zone after a certain period of abrasion. Despite having a higher hardness, TiC particles did not exhibit the same level of wear resistance as hBN particles. In the study, the best wear resistance result was obtained with equal proportions of hBN and TiC reinforcement. This is due to the high hardness behavior of the TiC particles and the formation of a tribo-layer to protect the metal matrix under the high wear temperature of the hBN particles. In pure Al sample, direct contact occurs between the abrasive pin and the wear surface. This combined effect leads to an increase in the amount of wear. The reduction in the wear rate of the hybrid composite with TiC and hBN reinforcement is due to the effective formation of a tribo-layer, which becomes thicker and denser as the wt% of hBN increases [52].

4 Conclusions

The homogeneously combined powders of hBN and TiC were pressed by cold pressing technique and sintered in a nitrogen atmosphere. The effects of additives on the microstructure, hardness, wear, and friction coefficient characteristics of the produced composites and the findings are presented below;

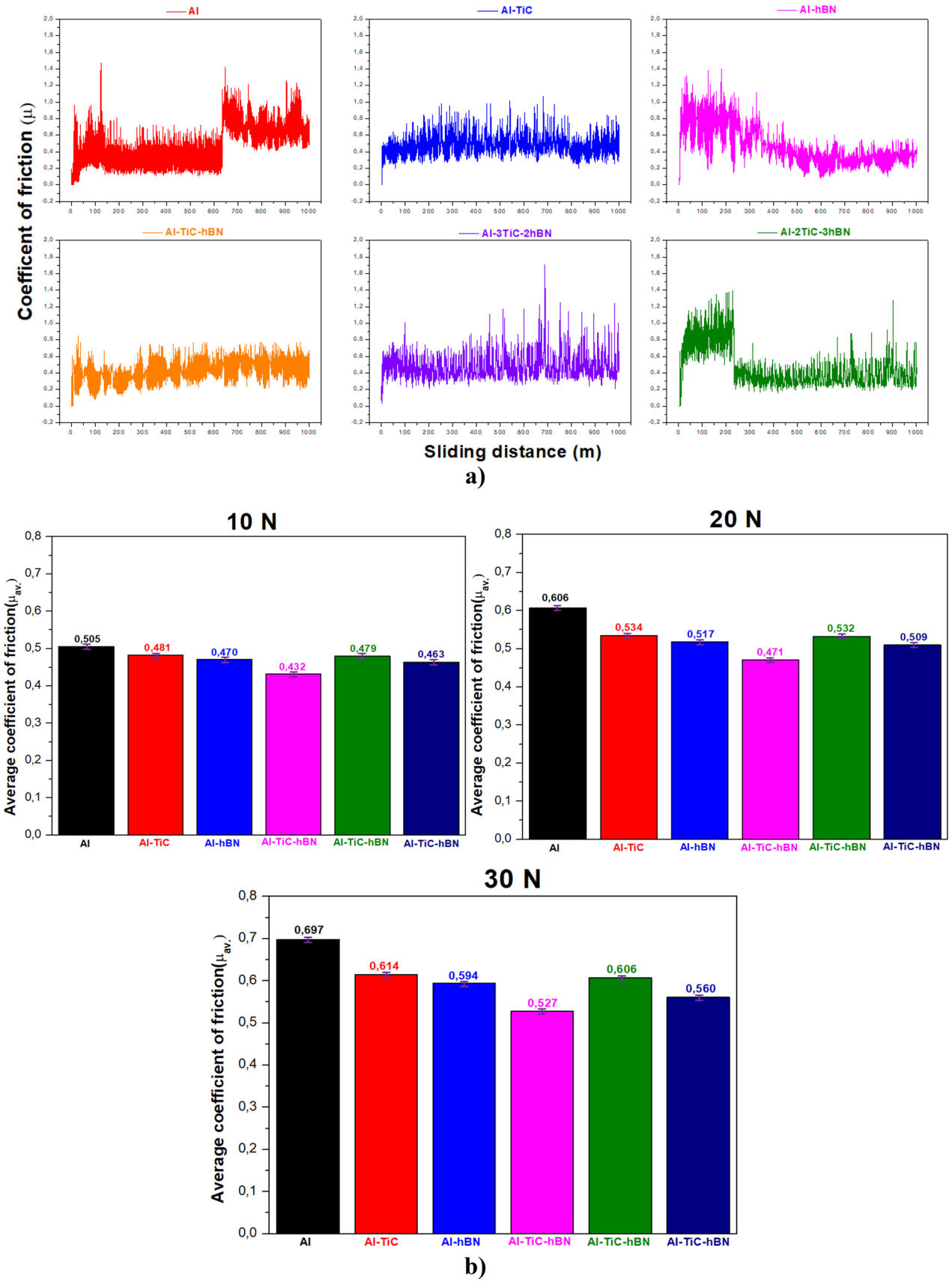

Fig. 13 Variation of friction coefficients with produced hybrid composites **a** coefficient of friction, **b** average coefficient of friction

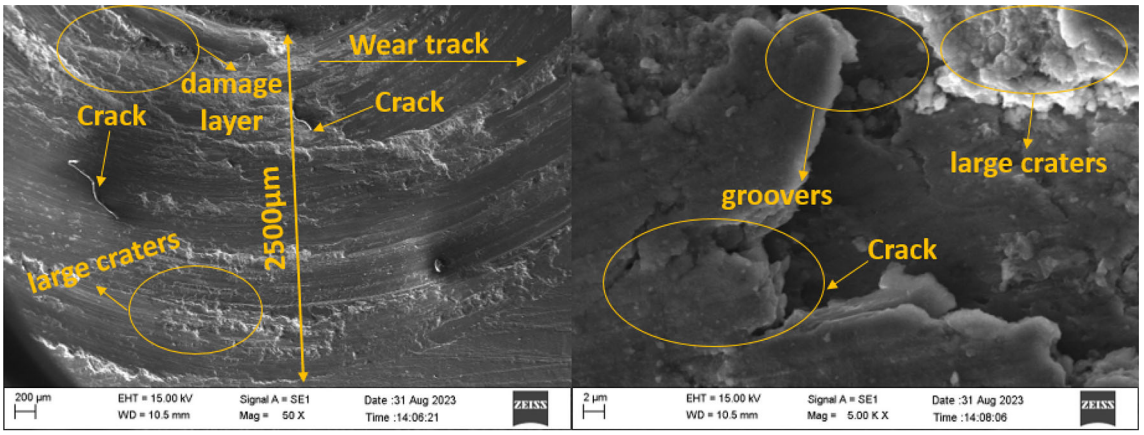

a)

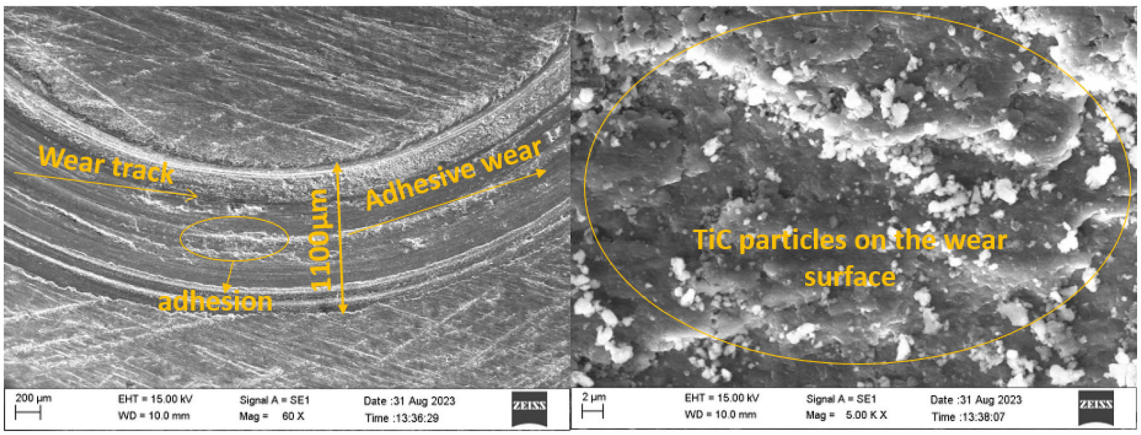

b)

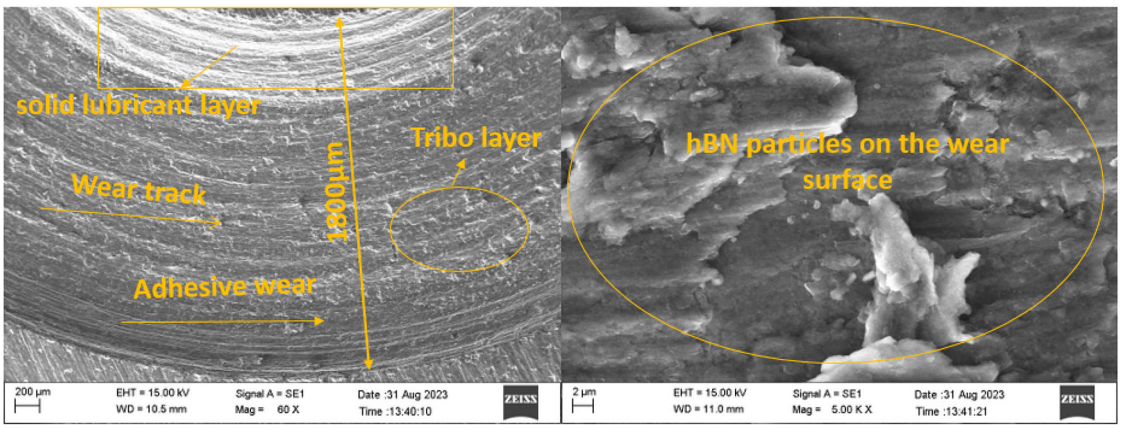

c)

Fig. 14 SEM images of wear of hybrid composites of **a** AL, **b** Al–TiC, **c** Al–hBN, **d** Al–TiC–hBN, **e** Al–3TiC–2hBN, **f** Al–2TiC–3hBN for 10 N

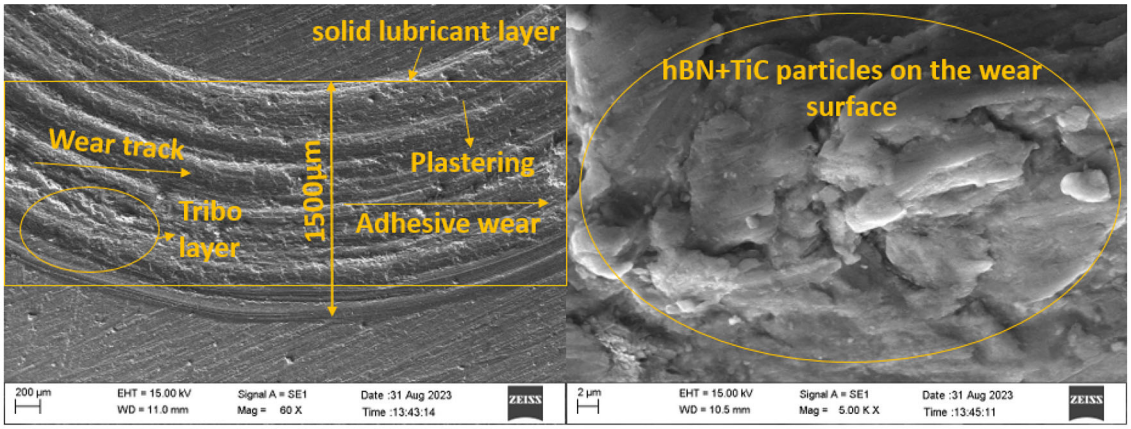

d)

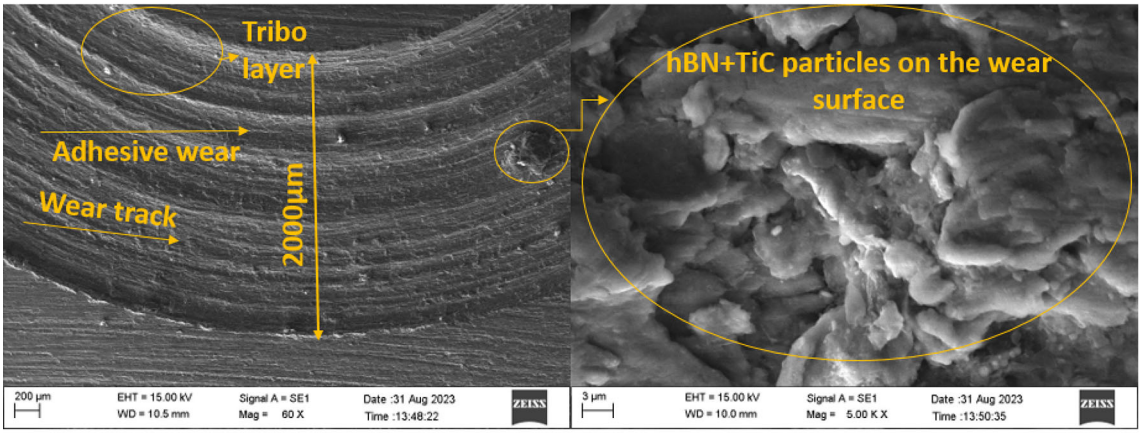

e)

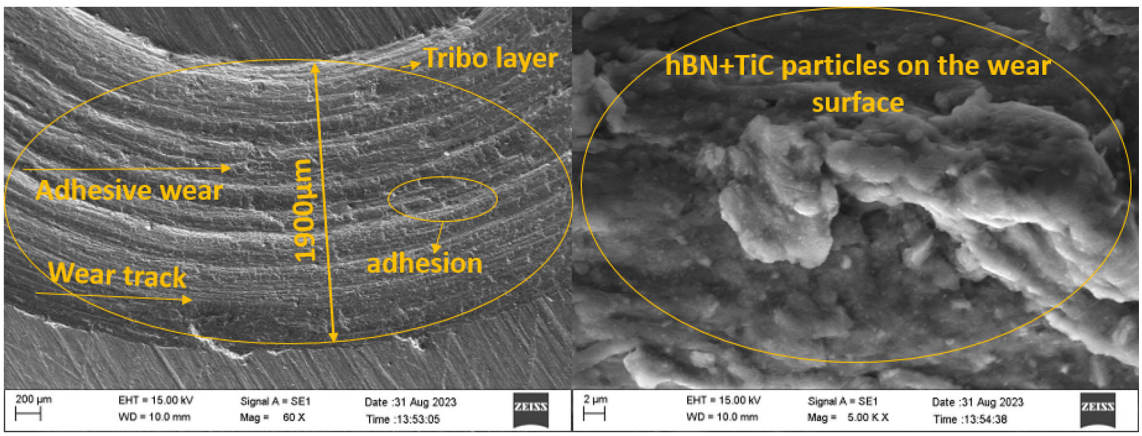

f)

Fig. 14 continued

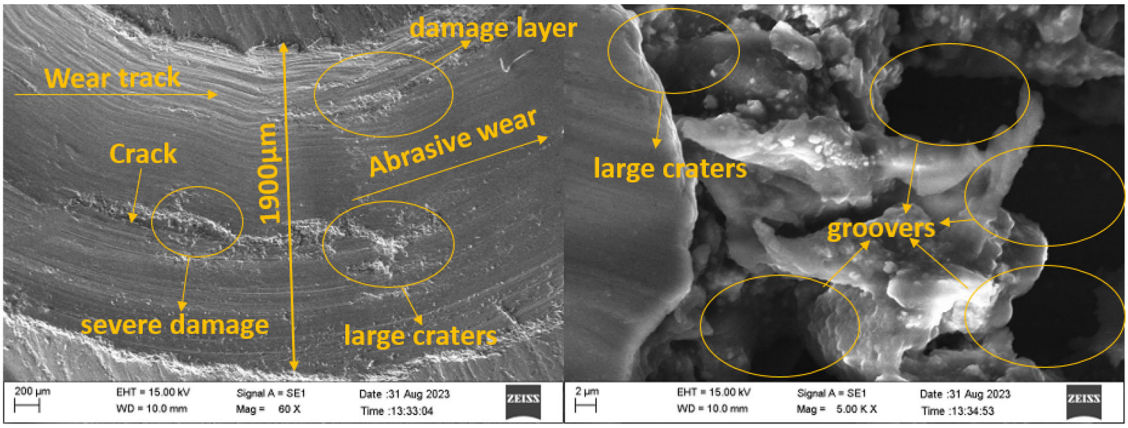

a)

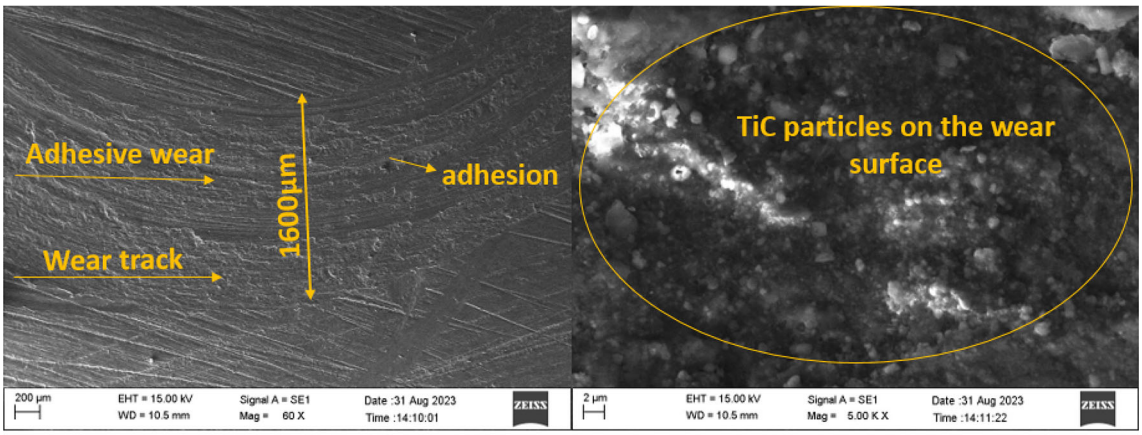

b)

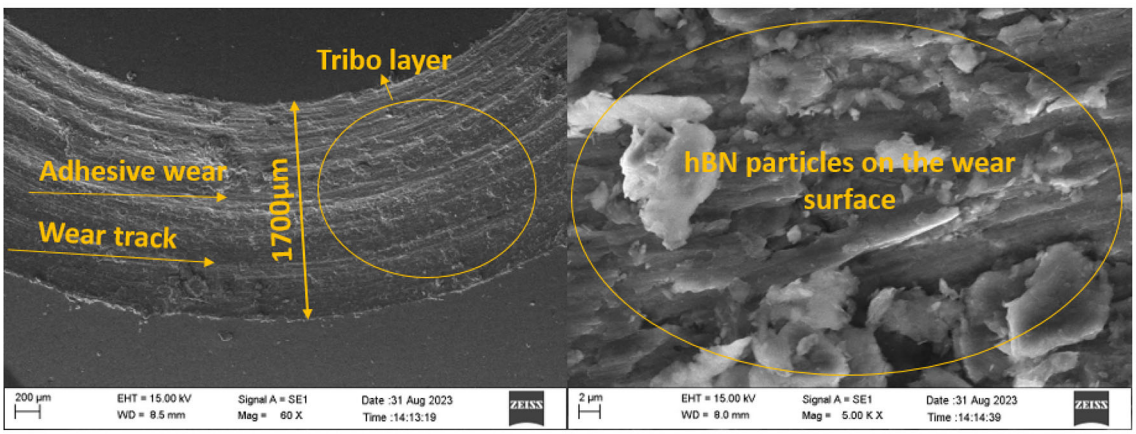

c)

Fig. 15 SEM images of wear of hybrid composites of **a** Al, **b** Al–TiC, **c** Al–hBN, **d** Al–TiC–hBN, **e** Al–3TiC–2hBN, **f** Al–2TiC–3hBN for 30 N

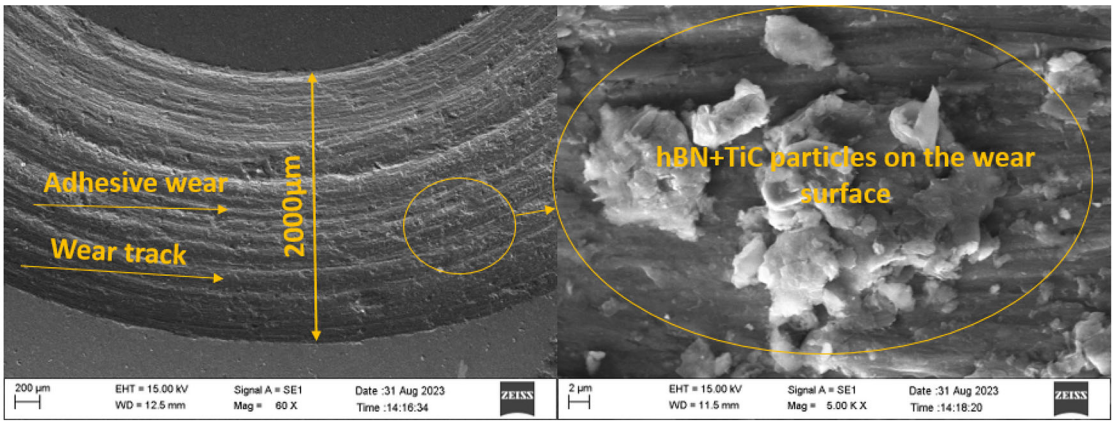

d)

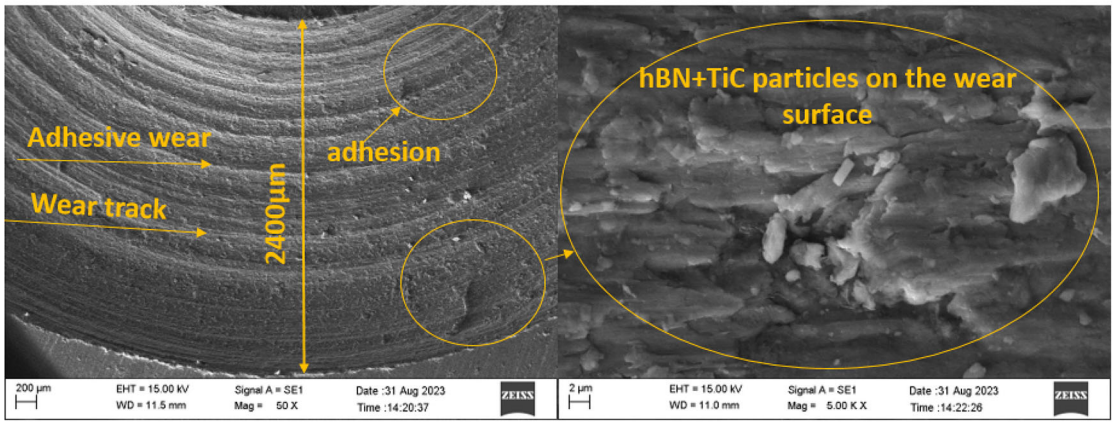

e)

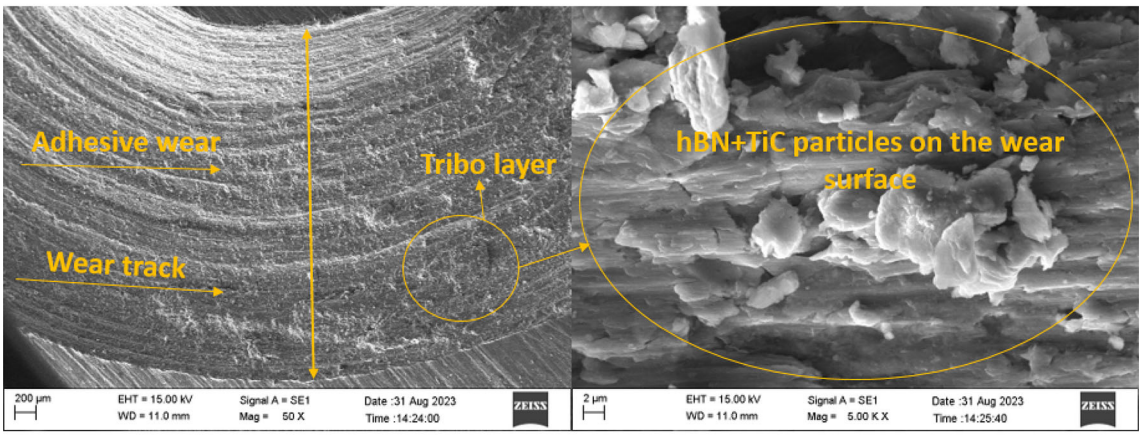

f)

Fig. 15 continued

- XRD examination revealed that Al–TiC–hBN particles maintained their unique phases while developing new compounds among themselves as a result of structural and morphological investigation. SEM images also showed that the reinforcing additives were dispersed within the matrix structure.
- The density value of the hybrid composites decreased with increasing hBN reinforcement.
- The hardness value increased significantly with all reinforcements compared to the pure Al sample.
- In wear tests, when compared to pure Al, the weight loss quantities and friction coefficient values of the composites improved significantly with the addition of TiC and hBN additions. The Al–TiC–hBN composite reinforced with TiC and hBN in equal amounts had the highest wear resistance and hardness value among all of the samples. It is believed that the findings from this study will allow for the utilization of longer-lasting machine parts in areas exposed to wear, as well as lower servicing costs in related industries.

Author Contributions The contributions of all authors to this paper: CKM contributed in performing the powder metallurgy process steps and wear tests; MH and BT contributed in studying the microstructure of the hybrid composites and completing their characterization; BA contributed in controlling, designing and writing the experiments. The manuscript has been read and approved in general terms by all authors.

Funding Open access funding provided by the Scientific and Technological Research Council of Türkiye (TÜBİTAK).

Data Availability Upon a reasonable request, the data that support this study's findings are available from the corresponding author.

Declarations

Conflict of interest The authors declare no competing interests.

References

1. Aslan, A.; Salur, E.; Düzcükoğlu, H.; Şahin, Ö.S.; Ekrem, M.: The effects of harsh aging environments on the properties of neat and MWCNT reinforced epoxy resins. Constr. Build. Mater. **272**, 121929 (2021)
2. Sepet, H.; Aydemir, B.; Tarakcioglu, N.: Evaluation of mechanical and thermal properties and creep behavior of micro-and nano-CaCO 3 particle-filled HDPE nano-and microcomposites produced in large scale. Polym. Bull. **77**, 3677–3695 (2020)
3. Umanath, K.; Palanikumar, K.; Selvamani, S.T.: Analysis of dry sliding wear behaviour of Al6061/SiC/Al2O3 hybrid metal matrix composites. Compos. Part B Eng. **53**, 159–168 (2013)
4. Salur, E.; Aslan, A.; Kuntoglu, M.; Gunes, A.; Sahin, O.S.: Experimental study and analysis of machinability characteristics of metal matrix composites during drilling. Compos. Part B Eng. **166**, 401–413 (2019)
5. Smagorinski, M.E.; Tsantrizos, P.G.; Grenier, S.; Cavasin, A.; Brzezinski, T.; Kim, G.: The properties and microstructure of Al-based composites reinforced with ceramic particles. Mater. Sci. Eng. A **244**, 86–90 (1998)
6. Zheng, R.; Hao, X.; Yuan, Y.; Wang, Z.; Ameyama, K.; Ma, C.: Effect of high volume fraction of B4C particles on the microstructure and mechanical properties of aluminum alloy based composites. J. Alloys Compd. **576**, 291–298 (2013)
7. Zhang, L.; Shi, J.; Shen, C.; Zhou, X.; Peng, S.; Long, X.: B4C-Al composites fabricated by the powder metallurgy process. Appl. Sci. **7**, 1009 (2017)
8. Abarghouie, S.M.R.M.; Reihani, S.M.S.: Investigation of friction and wear behaviors of 2024 Al and 2024 Al/SiCp composite at elevated temperatures. J. Alloys Compd. **501**, 326–332 (2010)
9. Ozay, C.; Ballikaya, H.; Dagdelen, F.; Karlidag, O.E.: Microstructural and wear properties of the Al-B4C composite coating produced by hot-press sintering on AA-2024 alloy. J. Mech. Sci. Technol. **35**, 2895–2901 (2021). https://doi.org/10.1007/s12206-021-0613-1
10. Tang, F.; Wu, X.; Ge, S.; Ye, J.; Zhu, H.; Hagiwara, M., et al.: Dry sliding friction and wear properties of B4C particulate-reinforced Al-5083 matrix composites. Wear **264**, 555–561 (2008)
11. Li, X.; Gao, Y.; Wei, S.; Yang, Q.: Tribological behaviors of B4C-hBN ceramic composites used as pins or discs coupled with B4C ceramic under dry sliding condition. Ceram. Int. **43**, 1578–1583 (2017)
12. Thakur, S.K.; Dhindaw, B.K.: The influence of interfacial characteristics between SiCp and Mg/Al metal matrix on wear, coefficient of friction and microhardness. Wear **247**, 191–201 (2001)
13. Hasırcı, H.; Gül, F.: Investigation of abrasive wear behaviours in B4C/Al composites depending on reinforcement volume fraction (2019)
14. Jiang, X.; Wang, N.; Zhu, D.: Friction and wear properties of in-situ synthesized Al2O3 reinforced aluminum composites. Trans. Nonferrous Metals Soc. China **24**, 2352–2358 (2014)
15. Mao, H.; Shen, F.; Zhang, Y.; Wang, J.; Cui, K.; Wang, H., et al.: Microstructure and mechanical properties of carbide reinforced TiC-based ultra-high temperature ceramics: a review. Coatings **11**, 1444 (2021)
16. Nagaral, M.; Hiremath, V.; Auradi, V.; Kori, S.A.: Influence of two-stage stir casting process on mechanical characterization and wear behavior of AA2014-ZrO2 Nano-composites. Trans. Indian Inst. Metals **71**, 2845–2850 (2018)
17. Akhtar, F.; Askari, S.J.; Shah, K.A.; Du, X.; Guo, S.: Microstructure, mechanical properties, electrical conductivity and wear behavior of high volume TiC reinforced Cu-matrix composites. Mater CharactCharact. **60**, 327–336 (2009)
18. Doğan, Ö.N.; Hawk, J.A.; Tylczak, J.H.; Wilson, R.D.; Govier, R.D.: Wear of titanium carbide reinforced metal matrix composites. Wear **225**, 758–769 (1999)
19. Zhong, L.; Xu, Y.; Hojamberdiev, M.; Wang, J.; Wang, J.: In situ fabrication of titanium carbide particulates-reinforced iron matrix composites. Mater. Des. **32**, 3790–3795 (2011)
20. Berns, H.; Wewers, B.: Development of an abrasion resistant steel composite with in situ TiC particles. Wear **251**, 1386–1395 (2001)

21. Fu, H.; Wu, X.; Li, X.; Xing, J.; Lei, Y.; Zhi, X.: Effect of TiC particle additions on structure and properties of hypereutectic high chromium cast iron. J. Mater. Eng. Perform. **18**, 1109–1115 (2009)
22. Mahathanabodee, S.; Palathai, T.; Raadnui, S.; Tongsri, R.; Sombatsompop, N.: Effects of hexagonal boron nitride and sintering temperature on mechanical and tribological properties of SS316L/h-BN composites. Mater. Des. **46**, 588–597 (2013)
23. Mahathanabodee, S.; Palathai, T.; Raadnui, S.; Tongsri, R.; Sombatsompop, N.: Dry sliding wear behavior of SS316L composites containing h-BN and MoS2 solid lubricants. Wear **316**, 37–48 (2014)
24. Hashim, F.A.; Abdulkader, N.J.; Jasim, N.S.: Effect of nano BN addition on the properties of an aluminum metal matrix composite. Eng. Technol. J. **36**, 691–695 (2018)
25. Sahoo, S.; Samal, S.; Bhoi, B.: Fabrication and characterization of novel Al-SiC-hBN self-lubricating hybrid composites. Mater. Today Commun. **25**, 101402 (2020)
26. Charoo, M.S.; Wani, M.F.: Tribological properties of h-BN nanoparticles as lubricant additive on cylinder liner and piston ring. Lubr. Sci. **29**, 241–254 (2017)
27. Tjong, S.C.; Lau, K.C.: Properties and abrasive wear of TiB2/Al-4% Cu composites produced by hot isostatic pressing. Compos. Sci. Technol. **59**, 2005–2013 (1999)
28. Xu, J.; Liu, W.: Wear characteristic of in situ synthetic TiB2 particulate-reinforced Al matrix composite formed by laser cladding. Wear **260**, 486–492 (2006)
29. Du, Z.M.; Li, J.P.: Study of the preparation of Al2O3sf· SiCp/Al composites and their wear-resisting properties. J. Mater. Process. Technol. **151**, 298–301 (2004)
30. Loganathan, P; Arivalagar, A.A; Nadanakumar, V; Paul, R.C; John, J.G.: Study on microstructure, mechanical and wear behavior of AA7075/hBN composites fabricated via liquid metallurgy. In: Proceedings. Materials Today (2023)
31. Singh, A.K.; Atheaya, D.; Tyagi, R.; Ranjan, V.: Friction and wear behavior of atmospheric plasma sprayed NiMoAl-Ag-hBN coatings at elevated temperatures. Surf. Coat. Technol. **466**, 129650 (2023)
32. Kumar, A.; Arafath, M.Y.; Gupta, P.; Kumar, D.; Hussain, C.M.; Jamwal, A.: Microstructural and mechano-tribological behavior of Al reinforced SiC–TiC hybrid metal matrix composite. Mater. Today Proc. **21**, 1417–1420 (2020)
33. Lu, Y.; Watanabe, M.; Miyata, R.; Nakamura, J.; Yamada, J.; Kato, H., et al.: Microstructures and mechanical properties of TiC-particulate-reinforced Ti–Mo–Al intermetallic matrix composites. Mater. Sci. Eng. A **790**, 139523 (2020)
34. Scaria, C.T.; Pugazhenthi, R.: Effect of process parameter on synthesizing of TiC reinforced Al7075 aluminium alloy nano composites. Mater. Today Proc. **37**, 1978–1981 (2021)
35. Saravanan, C.; Subramanian, K.; Anandakrishnan, V.; Sathish, S.: Tribological behavior of AA7075-TiC composites by powder metallurgy. Ind. Lubr. Tribol. **70**, 1066–1071 (2018)
36. Vairamuthu, J.; Senthil Kumar, A.; Stalin, B.; Ravichandran, M.: Optimization of powder metallurgy parameters of TiC-and B4C-reinforced aluminium composites by Taguchi method. Trans. Can. Soc. Mech. Eng. **45**, 249–261 (2020)
37. Hasan, F.; Jaiswal, R.; Kumar, A.; Yadav, A.: Effect of TiC and graphite reinforcement on hardness and wear behaviour of copper alloy B-RG10 composites fabricated through powder metallurgy. JMST Adv. **4**, 1–11 (2022)
38. Kumar, A.; Kumar, S.; Mukhopadhyay, N.K.; Yadav, A.; Winczek, J.: Effect of SiC reinforcement and its variation on the mechanical characteristics of AZ91 composites. Materials (Basel) **13**, 4913 (2020)
39. Mohazzab, P.: Archimedes' principle revisited. J. Appl. Math. Phys. **5**, 836–843 (2017)
40. Pradeep Devaneyan, S.; Ganesh, R.; Senthilvelan, T.: On the mechanical properties of hybrid aluminium 7075 matrix composite material reinforced with SiC and TiC produced by powder metallurgy method. Indian J. Mater. Sci. (2017)
41. Rahman, M.H.; Al Rashed, H.M.M.: Characterization of silicon carbide reinforced aluminum matrix composites. Procedia Eng. **90**, 103–109 (2014)
42. Kumar, G.B.V.; Rao, C.S.P.; Selvaraj, N.: Mechanical and tribological behavior of particulate reinforced aluminum metal matrix composites—a review. J. Miner. Mater. Charact. Eng. **10**, 59 (2011)
43. Paulraj, P.; Harichandran, R.: The tribological behavior of hybrid aluminum alloy nanocomposites at high temperature: role of nanoparticles. J. Mater. Res. Technol. **9**, 11517–11530 (2020)
44. Liu, L.; Li, W.; Tang, Y.; Shen, B.; Hu, W.: Friction and wear properties of short carbon fiber reinforced aluminum matrix composites. Wear **266**, 733–738 (2009)
45. Ramesh, C.S.; Pramod, S.; Keshavamurthy, R.: A study on microstructure and mechanical properties of Al 6061–TiB2 in-situ composites. Mater. Sci. Eng. A **528**, 4125–4132 (2011)
46. Baskaran, S.; Anandakrishnan, V.; Duraiselvam, M.: Investigations on dry sliding wear behavior of in situ casted AA7075–TiC metal matrix composites by using Taguchi technique. Mater. Des. **60**, 184–192 (2014)
47. Cabeza, I.; Merino, P.; Pena, G.; Pérez, M.C.; Cruz, S.V.; Rey, P.M.F.: Effect of high energy ball milling on the morphology, microstructure and properties of nano-sized TiC particle-reinforced 6005A aluminium alloy matrix composite. Powder Technol. **321**, 31–43 (2017). https://doi.org/10.1016/j.powtec.2017.07.089
48. Ramkumar, K.R.; Bekele, H.; Sivasankaran, S.: Experimental investigation on mechanical and turning behavior of AL 7075/x% wt. TiB 2-1% Gr in situ hybrid composite. Adv. Mater. Sci. Eng. (2015)
49. Subbarayan, R.; Al-Mufadi, F.A.; Siddharth, S.; Raghu, R.: Investigations on microstructure, mechanical, and tribological behaviour of AA 7075–x wt.% TiC composites for aerospace applications. Arch. Civ. Mech. Eng. **19**, 428–438 (2019). https://doi.org/10.1016/j.acme.2018.12.003
50. Chen, B.; Bi, Q.; Yang, J.; Xia, Y.; Hao, J.: Tribological properties of solid lubricants (graphite, h-BN) for Cu-based P/M friction composites. Tribol. Int. **41**, 1145–1152 (2008)
51. Tyagi, R.; Xiong, D.; Li, J.; Dai, J.: High-temperature friction and wear of Ag/h-BN-containing Ni-based composites against steel. Tribol. Lett. **40**, 181–186 (2010)
52. Ayyanar, S.; Gnanavelbabu, A.; Rajkumar, K.; Loganathan, P.: Studies on high temperature wear and friction behaviour of AA6061/B4C/hBN hybrid composites. Metals Mater. Int. **27**(8), 3040–3057 (2021)